

Arrays of microlenses of complex shapes prepared by reaction-diffusion in thin films of ionically doped gels

Christopher J. Campbell, Eric Baker, Marcin Fialkowski, and Bartosz A. Grzybowski^{a)}

Department of Chemical and Biological Engineering, Northwestern University, 2145 Sheridan Road, Evanston, Illinois 60208

(Received 16 April 2004; accepted 29 June 2004)

This letter describes a wet-stamping technique for the fabrication of highly regular arrays of microlenses through reaction-diffusion-swelling processes occurring in a thin film of ionically doped gelatin. Geometrical parameters of the lenses depend on and can be controlled by the geometries of the stamped features and the concentrations of chemicals diffusing and reacting in the gelatin matrix. Surface topographies of the lenses are studied experimentally, and are reproduced by a lattice gas reaction-diffusion model. © 2004 American Institute of Physics.

[DOI: 10.1063/1.1787595]

Microlenses are important components of several optical technologies. Individual microlenses find uses in fiber optics,¹ optical data storage,² and medical devices.³ Regular arrays of microlenses, on the other hand, are found in imaging sensors,⁴ optical limiters,⁵ confocal microscopy,⁶ and quantum computing systems.⁷ Several methods of making such arrays have been developed in recent years. Conventional ones, based on photolithography and/or micromachining, require the use of specialized equipment and usually involve several registration steps.^{8,9} Alternative, often very elegant fabrication schemes combine soft lithographic techniques and self-assembly and rely on either differential dewetting of a liquid prepolymer (subsequently to being cured into solid lenses) from a chemically micropatterned surface¹⁰ or on a templated assembly of microspheres on such a surface.¹¹ The de-wetting method is, however, limited by the interfacial properties of the polymer used (determining the curvature of the resultant lens), and the self-assembly approach has so far been limited to arrays of spherical lenses. In this letter, we describe a versatile and reliable method of fabrication of highly regular arrays of microlenses—with areas of up to 3×3 cm—of various symmetries and curvatures by means of reaction-diffusion (RD) processes^{12,13} occurring in a thin layer of an ionically doped gel. This method uses agarose stamps patterned in bas-relief to locally deliver a solution of silver nitrate AgNO_3 onto a surface of dry gelatin doped with potassium hexacyanoferrate, $\text{K}_4\text{Fe}(\text{CN})_6$. Precipitation reaction between silver cations diffusing into gelatin and hexacyanoferrate anions therein results in a pronounced expansion of the gel—the degree of this expansion is proportional to the amount of precipitate formed at a given location. The surface topographies obtained by RD in gelatin can be faithfully transferred into a polymeric replica serving as a microlens array.

Figure 1(a) outlines the experimental procedure. A hot, degassed 8 % w/w solution of agarose (OmniPur Agarose, Darmstadt, Germany) in de-ionized water was cast against an oxidized poly(dimethyl siloxane) master having an array of raised features embossed on its surface ($50\text{--}150\ \mu\text{m}$ in diameter, D). After gelation, the agarose layer was gently peeled off, and cut into $\sim 2\ \text{cm} \times 2\ \text{cm}$ rectangular blocks

(stamps) patterned with an array of depressions in bas relief. The stamps were soaked in a solution of AgNO_3 (typically, $0.65\text{--}1.50\ \text{M}$) for 12 h. Immediately prior to stamping, each stamp was dried on a tissue paper for 120 s, and applied onto

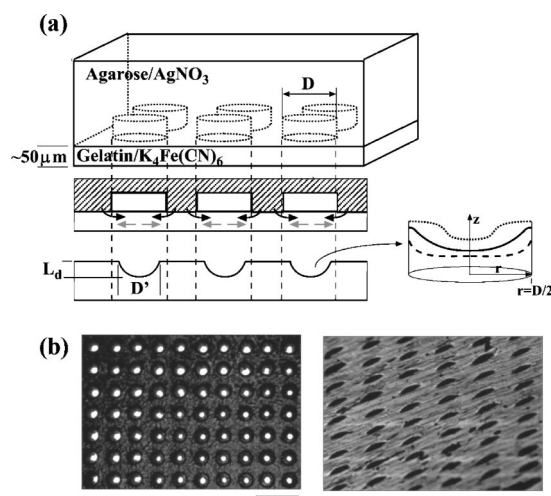


FIG. 1. (a) Top picture is the scheme of the experimental setup. Middle picture shows an agarose stamp (denoted with hatched lines) placed in contact with gelatin at $t=0$. The arrows indicate the directions of diffusion of Ag^+ cations (black arrows) and $\text{Fe}(\text{CN})_6^-$ anions (gray arrows). Bottom: After the stamp is taken off ($t=20$ min), and gelatin is allowed to dry ($t=6\text{--}7$ h), the regions between the stamped features appear as curvilinear depressions on the gelatin's surface. The dimensions of these depressions, D' and L_d , depend on the size of the stamped features, and on the concentrations of the salts used. The graph on the right shows qualitative trends observed with increasing salt concentrations. As $[\text{K}_4\text{Fe}(\text{CN})_6]$ or $[\text{AgNO}_3]$ are increased (from dashed to solid to dotted lines), the degree of gel swelling in the regions below and around the features increases; at the same time, the reaction fronts propagate more and more inwards lifting the central portion of the circle. Above certain concentration (here, above that corresponding to the solid line), the dimensions of the depressions—that is, D' and L_d —start decreasing. (b) Optical micrograph of an array of circularly symmetric depressions ($D=50\ \mu\text{m}$, $D' \approx 45\ \mu\text{m}$, 10% w/w AgNO_3 , 1% w/w $\text{K}_4\text{Fe}(\text{CN})_6$) in the gelatin master (left), and a SEM image of the corresponding array of microlenses on the surface of a PDMS replica. The scale bars correspond to $200\ \mu\text{m}$. The geometries of microlenses in this and other arrays—with exception of large circles and/or low salt concentrations—were well-approximated by the sections of a sphere, and their focal lengths agreed with those calculated using the spherical approximation. For the array shown here replicated in PDMS ($n=1.43$)—Refs. 18 and 19, the focal length was measured at $\sim 82 \pm 5\ \mu\text{m}$ compared to the calculated value of $75\ \mu\text{m}$.

^{a)} Author to whom correspondence should be addressed; electronic mail: grzybor@northwestern.edu

a $d_0 \sim 50\text{-}\mu\text{m}$ -thick film of dry gelatin (Gelatin B, 225 bloom, Sigma-Aldrich) doped with 0.25–1.0% w/w of $\text{K}_4\text{Fe}(\text{CN})_6$. After $t=20$ min, the stamp was removed from the wetted/swollen gelatin surface. This surface was left to dry for 6–7 h under ambient conditions ($T \sim 25^\circ\text{C}$, $RH \sim 20\% - 40\%$) to give an array of regular, curvilinear depressions in the regions corresponding to the depressions in the applied stamp. PDMS (Sylgard 184, Dow Corning) was cast against this surface, cured at 30 deg overnight, and peeled off to give an optically transparent material with an array of convex microlenses on its surface.

When the top portions of the features in the stamp come into conformal contact with the surface of the gelatin, water and ions diffuse from the stamp into the gel.^{12,13} The evolution of the surface topography upon stamping can be qualitatively explained by the diffusion of Ag^+ and $\text{Fe}(\text{CN})_6^{4-}$ ions in wetted gelatin and by the gel swelling due to the precipitation of these ions to give $\text{Ag}_4\text{Fe}(\text{CN})_6$ [Fig. 1(a), lowest picture and the inset on the right; also cf. EPAPS Ref. 14]. Initially, water from the stamp wets the surface of dry gelatin by capillarity, and slowly diffuses into its bulk.¹³ When silver cations enter the wetted gel, they are instantaneously precipitated in the reaction with $\text{Fe}(\text{CN})_6^{4-}$ present therein. More cations are diffusively resupplied from the stamp, but the rate of their delivery through the agarose–gelatin interface decays exponentially with time.¹² As the reaction (precipitation) front propagates away from the features, the unreacted $\text{Fe}(\text{CN})_6^{4-}$ experiences a sharp concentration gradient at this front and diffuses in its direction; the combination of these two, spatially opposite diffusive processes translates into the concentration of the precipitate monotonically decaying with the distance from the features; this concentration profile is, in turn, proportional to the degree of surface deformation. The reaction and diffusion phenomena continue until either (i) all $\text{Fe}(\text{CN})_6^{4-}$ in the gelatin has been used, or (ii) the elastic potential energy of the swollen gel exceeds the favorable energy of gel wetting.

Since local deformations of the gel surface depend on the local concentrations of diffusing and reacting salts, we expected that the topographies of the depressions in the gelatin master (or, equivalently, of the lenses in the PDMS replica) should depend on the dimensions of the stamped features and/or on concentrations of the salts used. These dependencies were studied using stamps micropatterned with arrays of circular posts (Fig. 2). We found that for given concentrations of participating chemicals, the depth of the lenses, L_d , increased with increasing diameter of the stamped circles D [all curves in Figs. 2(a) and 2(b)] until it reached a plateau at $D \sim 150\text{--}200\ \mu\text{m}$ — in this limit, the precipitation front from the perimeter of the circle did not propagate all the way to the circle's center, and L_d depended solely on the degree of swelling directly below the features. In addition, increasing D decreased the curvature of the lenses: in large circles, the central area where no precipitation occurred remained flat.

For a given D , the topographies of lenses could be controlled by concentrations of the salts in the stamp and in the gelatin. With $[\text{AgNO}_3]$ kept constant [Fig. 2(a)], L_d increased with increasing $[\text{K}_4\text{Fe}(\text{CN})_6]$ up to 1% w/w (above this concentration, the gelatin did not gelate properly and tended to “melt” when stamped upon). This trend reflected the fact that the more potassium hexacyanoferrate that was available in

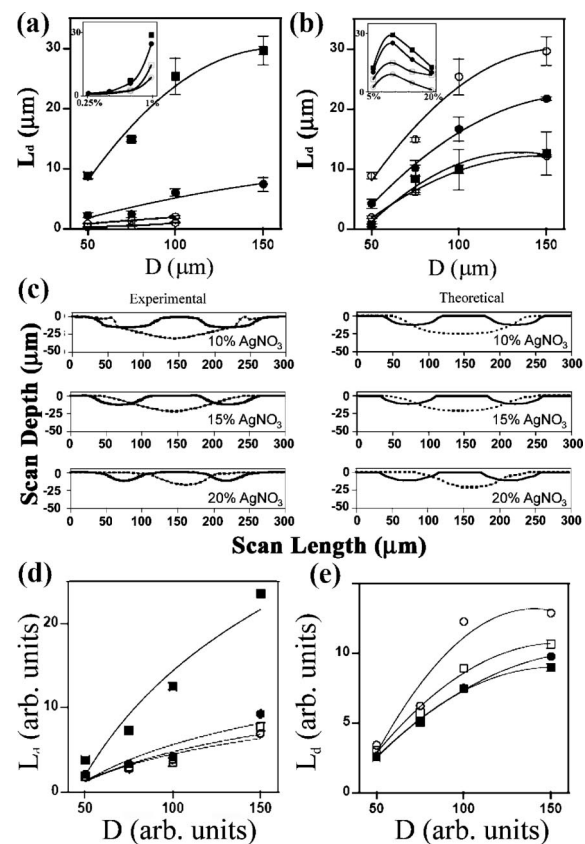


FIG. 2. (a) Experimental dependence of the depth, L_d , of circularly symmetric depressions on feature size, D , for varying concentrations of $\text{K}_4\text{Fe}(\text{CN})_6$ in gelatin [(○) 0.25%, (□) 0.5%, (●) 0.75%, (■) 1.0%] and for a constant concentration of AgNO_3 in the stamp (10%). Inset shows the same data plotted against $[\text{K}_4\text{Fe}(\text{CN})_6]$ for different values of D [(○) 50 μm , (□) 75 μm , (●) 100 μm , (■) 150 μm]. (b) L_d as a function of D for $[\text{K}_4\text{Fe}(\text{CN})_6] = 1\%$ w/w and for $[\text{AgNO}_3]$ varying from 5% to 20% [(□) 5%, (○) 10%, (●) 15%, (■) 20%]. Inset shows the same data plotted against $[\text{AgNO}_3]$ for different values of D [(○) 50 μm , (□) 75 μm , (●) 100 μm , (■) 150 μm]. Graphs in (a) and (b) were created based on profilometric measurements of the gelatin masters. Standard deviations are reported for the depths of the microlenses, and were collected from at least three independent stampings with two profilometric scans (averaged over ten times each) spanning two to five features for each stamping. For lenses with $D < 100\ \mu\text{m}$, the standard deviations for the depths and widths of the microlenses were less than 1%. (c) Experimental (left) and modeled (right) surface profiles for circular depressions $D = 75\ \mu\text{m}$ (solid line) and $D = 150\ \mu\text{m}$ (dashed line) for varying concentrations of silver nitrate and for 1% w/w $\text{K}_4\text{Fe}(\text{CN})_6$ in gelatin. (d) Theoretical dependence of L_d on D (both in arbitrary units) for varying concentrations of $\text{K}_4\text{Fe}(\text{CN})_6$ in gelatin [(○) 0.75, (□) 1.5, (●) 2.25, (■) 3] and with constant $[\text{AgNO}_3] = 50$ in the stamp. (e) Theoretical dependence of L_d on D for varying concentrations of AgNO_3 in the stamp [(■) 25, (○) 50, (□) 75, (●) 100] and for $[\text{K}_4\text{Fe}(\text{CN})_6] = 3$ (arbitrary units). Each data point in (d) and (e) is an average of 50 simulation runs performed with $\lambda = 2$, $D_A/D_B = 0.3$, $c = 4$; $W_0 = 510$. In all simulations, the concentrations were in arbitrary units that, however, were linearly proportional to the experimental concentrations. The 10% experimental concentration of AgNO_3 was assigned a numerical value of 50 in the simulations, and 1% w/w concentration of potassium hexacyanoferrate corresponded to 3.

the gelatin, the more precipitate could form, and the higher the degree of swelling.¹⁴ Also, the increasing concentration of $\text{K}_4\text{Fe}(\text{CN})_6$ decreased the effective diameter of the lens, D' , and increased surface curvature. These effects can be explained by the extent of the propagation of the precipitation front inwards [cf. the inset to Fig. 1(a)]: when $[\text{K}_4\text{Fe}(\text{CN})_6]$ was low, all ions were precipitated below and in the vicinity of the stamped ring and only these regions developed curvature; when more hexacyanoferrate was avail-

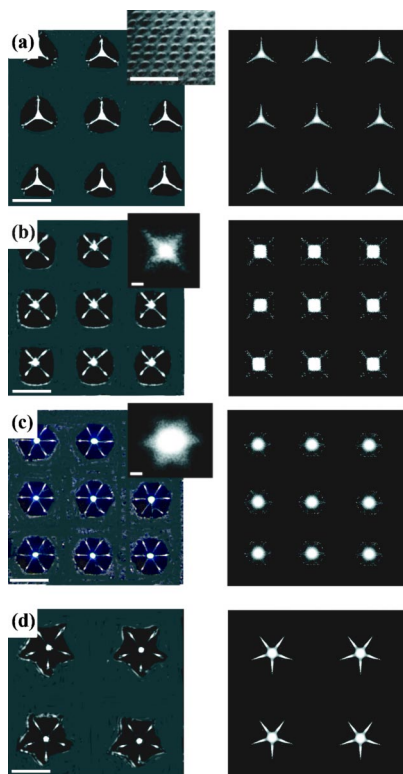


FIG. 3. Microlenses of complex base shapes: (a) triangular, (b) square, (c) hexagonal, and (d) pentagonal stars. The left column shows the optical micrographs ($[\text{K}_4\text{Fe}(\text{CN})_6]=1\%$ w/w, $[\text{AgNO}_3]=10\%$), while the right one has the results of the numerical simulations performed with $A(n=0)=3$, $B=50$, $\lambda=2$, $D_A/D_B=0.3$, $c=4$; $W_0=510$. The insert to (a) illustrates a long-range order in the stamped array of triangles. Insets to (b) and (c) are the images of the focal plane of the corresponding lens arrays. Scale bars in the primary pictures in (a)–(d) correspond to $150\ \mu\text{m}$; those in the inserts are $1\ \text{mm}$ in (a) and $2\ \mu\text{m}$ in (b) and (c).

able, the front traveled further, curving the center of the circle and leaving behind itself a flat region of uniform precipitation.

The effects of silver nitrate concentration on the topography of the surface were studied over a wider range of concentrations, 5%–20% [Fig. 2(b); higher concentrations dissolved gelatin supports]. For relatively low concentrations ($< \sim 10\%$), L_d increased with increasing $[\text{AgNO}_3]$ (a trend similar to that observed when $[\text{K}_4\text{Fe}(\text{CN})_6]$ was increased), but the lenses were relatively flat-bottomed. Curved lenses were obtained when the concentration was above $\sim 10\%$. In this regime, however, L_d decreased with increasing $[\text{AgNO}_3]$. This trend was due to the reaction fronts reaching the center of a lens, precipitating $\text{Fe}(\text{CN})_6^{4-}$ still present therein and lifting this region up with respect to the perimeter of the lens¹⁴ [Fig. 2(c)].

The technique was straightforwardly extended to arrays of microlenses of arbitrary base shapes. Figure 3 shows optical micrographs of “pyramidal” lenses obtained by stamping arrays of triangles [Fig. 3(a)], squares [Fig. 3(b)], and hexagons [Fig. 3(c)]. When star patterns were stamped, they produced intricate multi-faceted surface reliefs [Fig 3(d)]. As in the case of circularly symmetric patterns, the topographic details of these reliefs could be controlled by the concentrations of the participating chemicals, and were faithfully re-

produced [Fig. 2(c) right column, Figs. 2(d) and 2(e), Fig. 3, right column] by a lattice gas model with reaction term algorithm.¹⁵ This model proved very useful in guiding the design of stamps and in selection of concentrations leading to desired buckled structures. Description of the modeling method is included in EPAPS Ref. 14, and the simulation software is available free of charge from our Web page.¹⁶

In summary, we have demonstrated that reaction-diffusion phenomena can be the basis of a reliable microfabrication method of technologically important microstructures. The technique we developed is simple, flexible, and allows a high degree of control over the topographies of surface reliefs it produces. The noncircular lenses (“micropyramids”) we prepared should be useful not only in wave-front-engineering,^{17,18} but also as brightness-enhancing supports in liquid crystal displays,¹⁹ and as microcontainers for crystallization.²⁰

B.G. gratefully acknowledges financial support from Northwestern University start-up funds and from the Camille and Henry Dreyfus New Faculty Awards Program. C.C. was supported in part by the NSF-IGERT program “Dynamics of Complex Systems in Science and Engineering” (DGE-9987577), and M.F. by the NATO Post-Graduate Fellowship.

¹C. Edwards, H. M. Presby, and C. Dragone, *J. Lightwave Technol.* **11**, 252 (1993).

²I. D. Nikolov, K. Goto, S. Mitsugi, Y. J. Kim, and V. I. Kavardikov, *Nanotechnology* **13**, 471 (2002).

³A. E. Guber and P. Wienenke, *Proc. SPIE* **2676**, 2 (1996).

⁴N. Daemen and H. L. Peek, *Philips J. Res.* **48**, 281 (1994).

⁵M. V. Gryaznowa, V. V. Danilov, M. A. Belyaeva, P. A. Shakhverdov, O. V. Chistyakova, and A. I. Khrebtov, *Opt. Spectrosc.* **92**, 614 (2002).

⁶E. M. McCabe, C. M. Taylor, and L. Yang, *Proc. SPIE* **4876**, 1 (2002).

⁷R. Dumke, M. Volk, T. Muther, F. B. J. Buchkremer, G. Birkl, and W. Ertmer, *Phys. Rev. Lett.* **89**, 097903 (2002).

⁸U. Koehler, A. E. Guber, W. Bier, M. Hecke, and T. Schaffer, *Proc. SPIE* **2687**, 18 (1996).

⁹P. Ruther, B. Gerlach, J. Goettert, M. Ilie, J. Mohr, A. Mueller, and C. Ossmann, *Pure Appl. Opt.* **6**, 643 (1997).

¹⁰M. H. Wu and G. M. Whitesides, *J. Math. Psychol.* **12**, 747 (2002).

¹¹Y. Xia, E. Kim, X.-M. Zhao, J. A. Rogers, M. Prentiss, and G. M. Whitesides, *Science* **273**, 347 (1996).

¹²M. Fialkowski, C. J. Campbell, I. T. Bensemann, and B. A. Grzybowski, *Langmuir* **20**, 3513 (2004).

¹³C. J. Campbell, R. Klajn, M. Fialkowski, and B. A. Grzybowski, *Adv. Mater.* (Weinheim, Ger.) (to be published).

¹⁴See EPAPS Document No. E-APPLAB-85-008435 for further discussions of gel swelling, precipitation in the gel, trends in lens topography, and the theoretical model described in the article. A direct link to this document may be found in the online article’s HTML reference section. the document may also be reached via the EPAPS homepage (<http://www.aip.org/pubservs/epaps.html>) or from <ftp.aip.org> in the directory/epaps/. See the EPAPS homepage for more information.

¹⁵*Lattice Gas Methods for Partial Differential Equations*, edited by G. D. Doolen (Addison-Wesley, New York, 1990).

¹⁶The executable program implementing the model, along with instructions, can be found at <http://dysa.northwestern.edu>.

¹⁷B. A. Grzybowski, D. Qin, and G. M. Whitesides, *Appl. Opt.* **38**, 2997 (1999).

¹⁸B. A. Grzybowski, S. T. Brittain, and G. M. Whitesides, *Rev. Sci. Instrum.* **70**, 2031 (1999).

¹⁹L. Liwei, T. K. Shia, and C.-J. Chiu, *J. Micromech. Microeng.* **10**, 395 (2000).

²⁰V. R. Thalladi and G. M. Whitesides, *J. Am. Chem. Soc.* **124**, 3520 (2002).